Contrast-Enhanced Ultrasound Imaging with Chirps: Signal Processing and Pulse Compression

Sevan Harput, James McLaughlan, David M. J. Cowell, and Steven Freear,

Ultrasonics and Instrumentation Group, School of Electronic and Electrical Engineering,

University of Leeds, Leeds, LS2 9JT, UK

E-mail: S.Harput@leeds.ac.uk

Abstract—**Contrast-enhanced ultrasound imaging creates one of the worst case scenarios for pulse compression due to depth and frequency dependent attenuation, high level of harmonic generation, phase variations due to resonance behavior of microbubbles, and increased broadband noise by microbubble destruction. This study investigates the feasibility of pulse compression with a matched filter in the existence of microbubbles with resonant behavior.**

Simulations and experimental measurements showed that the scattered pressure from a microbubble population excited by a chirp waveform preserves its chirp rate even for harmonic frequencies. Although, pulse compression by a matched filter was possible due to the conservation of the chirp rate, an increase on sidelobe levels were observed at fundamental and second harmonic frequencies. Therefore, using chirp excitation and a matched filter pair will increase the contrast-to-tissue ratio with a trade-off of decreased image quality.

Index Terms—**Microbubbles, chirp coded excitation, linear frequency modulation, pulse compression, matched filter**

I. INTRODUCTION

It has been demonstrated that the microbubble response to wideband and long duration excitation is stronger [1], [2]. Since most commercial contrast agents have a polydisperse size distribution [3], [4], more microbubbles can be excited close to their resonance frequency. The microbubble behavior near resonance increases their scattering, which can achieve a better separation between tissue and contrast agents, thus a better contrast-to-tissue ratio (CTR).

The linear scattering behavior of microbubbles increases the CTR by improving the response from blood pools, vessels, and heart. Nevertheless, the nonlinear behavior of the microbubbles must be used to achieve a better separation between tissue and contrast agents [5]. In capillaries or small blood vessels, it is hard to detect microbubbles with their linear scattering response. However, increasing the pressure level will cause microbubbles to behave nonlinearly, which will allow the differentiation of their response from that of tissue [6]. These higher-order harmonic components generated due to nonlinear scattering from ultrasound contrast agents can be used in harmonic and superharmonic imaging [7], [8]. Bouakaz *et al.* demonstrated that the contrast-to-tissue ratio and image resolution can be improved by using higher-order harmonics generated by microbubbles [9].

Current research on ultrasound contrast imaging mostly focuses on exploiting the nonlinear behavior of the microbubbles
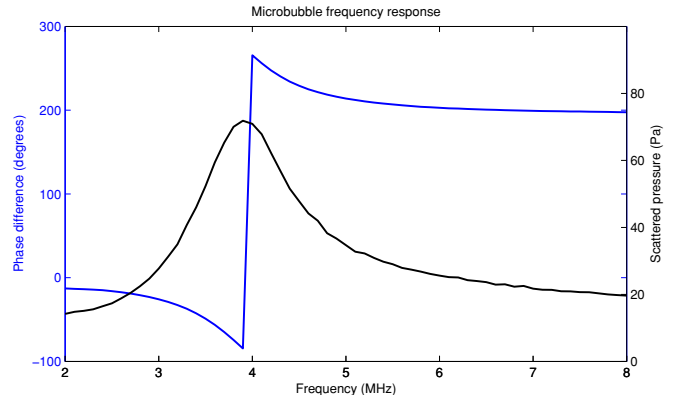

Fig. 1. Frequency response of a single microbubble with a resonance frequency of 3.8 MHz simulated with the Marmottant model.

[10]–[12]. Microbubbles excited with a chirp waveform generate more harmonics than with a sinusoidal tone burst of same duration. Although chirp excitation amplifies the microbubble response and offers an improved CTR, the resonance behavior of microbubbles introduces new complications for imaging applications. For this reason, this study investigates the effect of the pulse compression with the matched filter for the simulated and measured behaviors of microbubbles.

II. DEFINITION OF THE PROBLEM

The frequency response of a single microbubble coated with a thin layer of phospholipid was simulated with the Marmottant's model [13]. The motivation behind this simulation is to emphasize the effect of nonlinear microbubble response on pulse compression.

Fig. 1 shows the resulting phase and amplitude response of a single microbubble excited between $2-8$ MHz with a peak-to-peak pressure of 100 kPa. Spectrum of the scattered pressure from this microbubble shows that the natural oscillation was at 3.8 MHz, which was chosen specifically to match the resonance peak of microbubbles used in experiments.

When microbubbles are excited with a chirp waveform around their resonance frequency, both the phase and amplitude response will be significantly different than that of the tissue. Microbubbles will oscillate with a phase difference for the excitation frequencies below or above their resonance peak. The resonance behavior affects the phase, frequency and

amplitude of echoes, so the matched filter technique does not work as efficiently with microbubbles as it works with linear reflectors. Therefore, the scattered echoes from microbubbles will have sudden phase and amplitude variations that reduce the pulse compression efficiency.

III. MATERIALS AND METHODS

A. Microbubble Manufacture

Lipids were prepared by mixing DPPC, DSPE-PEG2000, and DPPA (Avanti Polar Lipids Inc., Alabaster, AL). Microbubbles were prepared by mixing these lipids in Dulbecco's Phosphate-Buffered Saline (DPBS) containing 1% glycerin and saturated with C_3F_8, which forms the gas core. The vial was shaken for 45 seconds by a CapMix mechanical shaker (3M ESPE, St. Paul, MN) [1], [14].

The microbubbles were diluted to $\sim 1 \times 10^6$ MB/ml to achieve similar concentrations to those observed in the human body during contrast imaging and to minimise multiple scattering effects. The resonance frequency of the microbubble population was measured as 3.8 MHz.

B. Pulse Compression with a Matched Filter

A linear frequency modulated (LFM) chirp can be represented as

$$s(t) = \cos(2\pi \left(f_0 t + \frac{\sigma}{2} t^2 \right)), \quad -\frac{T}{2} \leq t \leq \frac{T}{2} \qquad (1)$$

where $s(t)$ is a real signal with a center frequency of f_0, sweeping bandwidth of B, duration of T, and chirp rate of $\sigma = B/T$.

To improve the sidelobe performance after compression and to reduce the spectral leakage, a window can be used to shape the envelope of the signal as;

$$x(t) = A(t) \cdot s(t), \qquad (2)$$

where $x(t)$ is the transmitted signal with an amplitude modulation of $A(t)$.

In this study, a matched filter was used for pulse compression of the LFM signals. The matched filter calculates the probability of the signal's presence by compressing the energy contained within the signal into a single pulse. Therefore, pulse compression with a matched filter provides a resolution approximately in the order of $1/B$ and a gain in SNR at the receiver [15].

In order to design an ideal receiver, the matched filter's impulse response must be equal to the complex conjugate time reversal of the transmitted signal. For the real signal $s(t)$, defined in Eq. (1), the impulse response of the matched filter is given by;

$$m(t) = A(t) \cdot s(-t). \qquad (3)$$

A second harmonic matched filter can be designed in a similar way by second order distortion model as [16], [17];

$$m_{2H}(t) = A(t) \cdot s^2(-t). \qquad (4)$$

The time-domain output of the pulse compression is the convolution of the input signal with the matched filter, which
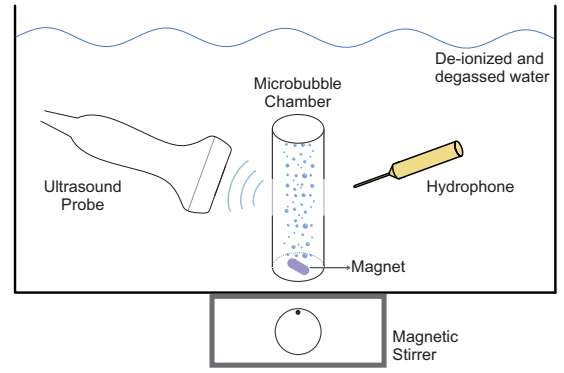

Fig. 2. Schematic diagram of the experimental setup for microbubble scattering measurements performed in a tank filled with de-ionized and degassed water. Measurements were performed with a commercial ultrasound probe connected to the UARP and a hydrophone.

is the autocorrelation function of the matched filter for an ideal case.

C. Experimental Setup for Scattering Measurements

Scattering measurements were performed to evaluate the microbubble response to LFM chirp excitation with different chirp rates. A L3-8/40EP medical probe (Prosonic Co., Korea) probe was used to replicate ultrasound imaging conditions during the measurements. The medical probe was used to excite the microbubbles in a cylindrical chamber with two acoustically transparent windows as shown in Fig. 2. A magnetic stirrer was used to ensure uniform microbubble distribution during the measurements.

In the experiments, three different LFM chirps were used for excitation. Chirp signals had a center frequency of 3.8 MHz, duration of 20 μs, and fractional bandwidths (FBWs) of 10%, 20%, and, 40%. A Hann window was applied over these signals to reduce spectral leakage [1]. The Ultrasound Array Research Platform (UARP) was used to generate these excitation waveforms [18].

The measurements were performed for a peak negative pressure range of $100 - 500$ kPa by renewing the microbubble suspension after five excitation. Scattered pressure waveforms from the contrast agents were received using a Polyvinylidene Difluoride (PVDF) 1 mm needle hydrophone (Precision Acoustics Ltd., Dorchester, UK), which was placed perpendicular to the ultrasound probe. The received signals were amplified by 40 dB using a 5072-PR pre-amplifier (Panametrics-NDT, Inc., Waltham, MA) and sampled with a 64xi Waverunner digital oscilloscope (LeCroy Corporation, Chestnut Ridge, NY) at 1 GHz. The frequency response of the hydrophone was corrected for during post processing in Matlab using the calibration data supplied by the National Physical Laboratory (Middlesex, UK). The received signals spectra were averaged in the frequency domain over the 150 measurements to reduce the variance of the experimental results and to show the average response from a microbubble population.
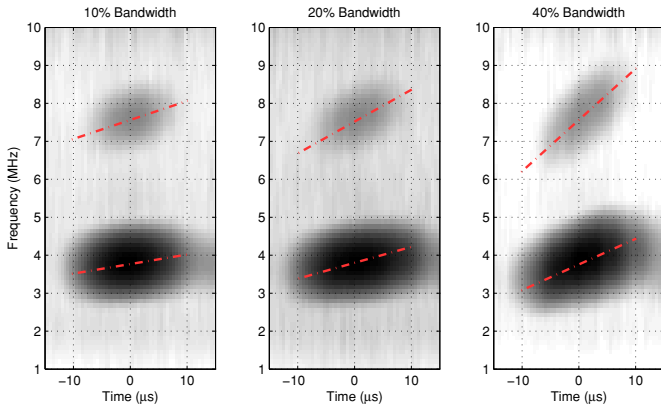
Fig. 3. Spectrogram of the scattered pressure from a microbubble population at 100 kPa excited by chirp waveforms with $f_0 = 3.8$ MHz, $T = 20$ μs, and fractional bandwidths of (Left) 10%, (Middle) 20%, and (Right) 40%. The red dashed lines show the theoretical center frequency and chirp rate of the fundamental and second harmonic components.
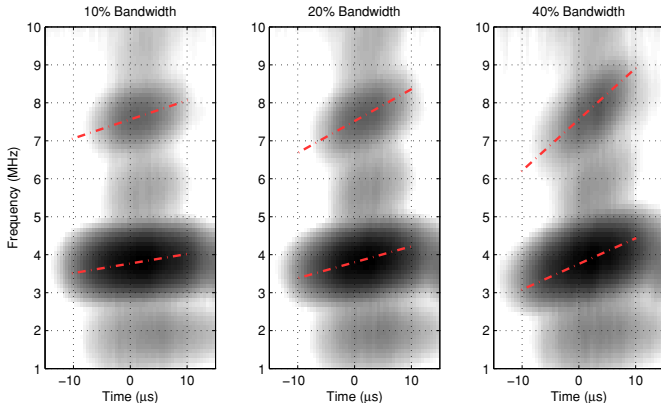

Fig. 4. Spectrogram of the scattered pressure from a microbubble population at 500 kPa excited by chirp waveforms with $f_0 = 3.8$ MHz, $T = 20$ μs, and fractional bandwidths of (Left) 10%, (Middle) 20%, and (Right) 40%. The red dashed lines show the theoretical center frequency and chirp rate of the fundamental and second harmonic components.

IV. RESULTS AND DISCUSSION

A. Scattering Response of a Microbubble Population

The motivation behind these measurements is to observe the effect of polydisperse microbubble size distribution and multiple scattering effects, where simulations were performed by solely focusing on the resonance behavior of microbubbles. For this reason, scattering response of diluted in-house microbubbles was measured for different excitation waveforms.

Fig. 3 and Fig. 4 show the spectral response of the scattered pressure from a population of microbubbles for different excitation waveforms. For chirp excitation with 10%, 20%, and 40% fractional bandwidths, scattered pressure waves maintained their chirp rates for the fundamental and harmonic components in all measurements performed between 100 kPa and 500 kPa, where only two measurements at each extremes of 100 kPa and 500 kPa were shown in Fig. 3 and Fig. 4. Even though the onset of harmonic generation and scattering at fundamental frequency varied for different measurements,
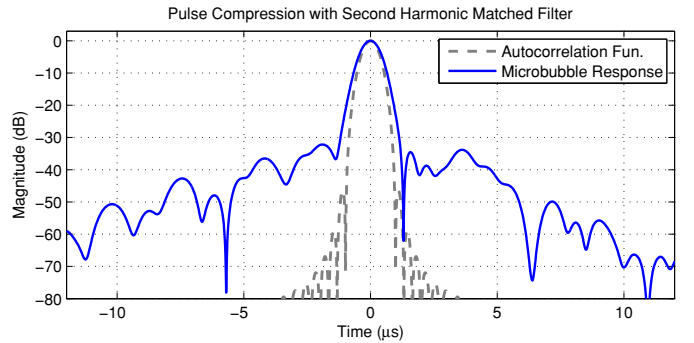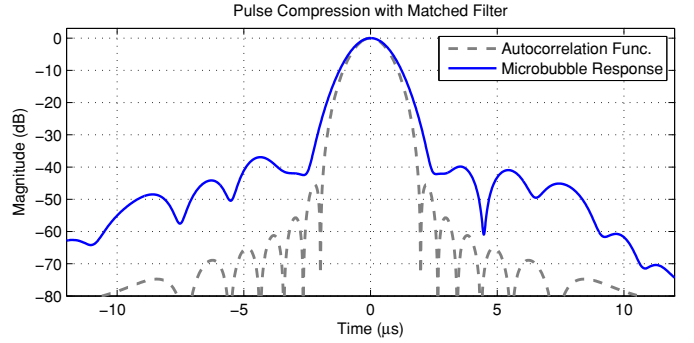

Fig. 5. Scattered pressure waveform compressed by (Top) a matched filter and (Bottom) a second harmonic matched filter. Dashed line is the autocorrelation function of the fundamental and the second harmonic matched filters given for comparison.

the fundamental and harmonic chirp rates were the same. The conservation of the chirp rate makes the pulse compression with a matched filter possible.

B. Response of a Single Microbubble

The response of a single microbubble with similar properties of that used in experiments was simulated with the Marmottant's model at 500 kPa [13]. Although microbubbles are highly echogenic and generate more harmonics than tissue even at low pressure levels, use of acoustic pressures as high as 500 kPa is common while imaging with microbubbles [19]. To simulate the amplitude deformations due to the frequency dependent attenuation a low pass filter with a slope of 0.5 dB/MHz was applied on the microbubble response.

The motivation behind this simulation is to show the feasibility of pulse compression for scattered pressure waves from a single microbubble excited with a LFM chirp near to its resonance of 3.8 MHz. The pulse compression was performed with a matched filter designed with the same parameters of the excitation signal; a center frequency of 3.8 MHz, a fractional bandwidth of 40%, and a duration of 20 μs. The pulse compression of the second harmonic component was performed with a second harmonic matched filter designed with twice the center frequency of excitation signal 7.6 MHz, a fractional bandwidth of 40% for the second harmonic frequency, and a duration of 20 μs.

Fig. 5 shows the simulated microbubble response compressed by (top) a matched filter and (bottom) a second

harmonic matched filter. The -6 dB mainlobe widths of both compressed fundamental and second harmonic signals were within 10% of their autocorrelation functions. As a result of resonance behavior of microbubbles and generation of harmonics by nonlinear microbubble oscillations, an increase in sidelobe levels was observed as high as -30 dB. The effect of this on the resulting ultrasound image will be reduced image quality, since high sidelobe levels decrease the resolution and create image artifacts.

V. Conclusions

Any dispersive media exhibits nonlinear behavior and generates harmonics. Yet, the mechanisms responsible for the nonlinear behavior of microbubbles are completely different. Tissue always generates harmonics in an expected manner, but microbubbles have unique acoustic signatures that change with size, shell composition, gas core, excitation pressure, and excitation frequency. However, the scattered response from the microbubble population still have the same chirp rate as the excitation signal and the chirp rate of the harmonics generated by the microbubbles are scaled by a ratio of n for the nth-harmonic as presented in spectrograms of measured microbubble responses. Although the chirp rate was preserved, the resonance behavior of microbubbles and generation of harmonics will reduce the image quality due to the increase in sidelobe levels after pulse compression.

The aim of contrast-enhanced ultrasound imaging is to be able to differentiate between perfused and non-perfused tissue, instead of imaging individual microbubbles with high quality and resolution. In terms of image contrast, chirp excitation will increase the scattering from polydisperse microbubbles [1], [2] and a matched filter will improve the SNR by compressing the scattered energy with a certain chirp rate into a single pulse [15]. Further improvement on image quality can be achieved by filtering and performing pulse compression with the fractional Fourier transform (FrFT) and the Fan Chirp Transform (FChT) techniques [20], [21]. Therefore, a pulse compression system with chirp excitation and a matched filter will maximize the CTR in contrast-enhanced ultrasound imaging at fundamental and harmonic frequencies with a trade-off of decreased image quality.

References

[1] S. Harput, M. Arif, J. McLaughlan, D. M. J. Cowell, and S. Freear, "The effect of amplitude modulation on subharmonic imaging with chirp excitation," *Ultrasonics, Ferroelectrics and Frequency Control, IEEE Transactions on*, vol. 60, no. 12, pp. 2532–2544, 2013.

[2] J. McLaughlan, N. Ingram, P. R. Smith, S. Harput, P. L. Coletta, S. Evans, and S. Freear, "Increasing the sonoporation efficiency of targeted polydisperse microbubble populations using chirp excitation," *Ultrasonics, Ferroelectrics and Frequency Control, IEEE Transactions on*, vol. 60, no. 12, pp. 2511–2520, 2013.

[3] J.-M. Gorce, M. Arditi, and M. Schneider, "Influence of bubble size distribution on the echogenicity of ultrasound contrast agents: A study of sonovue," *Investigative Radiology*, vol. 35, no. 11, pp. 661–671, 2000.

[4] D. E. Goertz, N. de Jong, and A. F. van der Steen, "Attenuation and size distribution measurements of definity and manipulated definity populations," *Ultrasound in Medicine & Biology*, vol. 33, no. 9, pp. 1376–1388, 2007.

[5] P. N. Burns, D. H. Simpson, and M. A. Averkiou, "Nonlinear imaging," *Ultrasound in Medicine & Biology*, vol. 26, no. 1, pp. 19–22, 2000.

[6] S. Harput, J. McLaughlan, P. R. Smith, D. M. J. Cowell, S. D. Evans, and S. Freear, "Separating the second harmonic response of tissue and microbubbles using bispectral analysis," in *IEEE Ultrasonics Symposium*, 2012, pp. 1930–1933.

[7] A. Bouakaz, S. Frigstad, F. J. T. Cate, and N. de Jong, "Super harmonic imaging: a new imaging technique for improved contrast detection," *Ultrasound in Medicine & Biology*, vol. 28, no. 1, pp. 59–68, 2002.

[8] S. Harput, J. McLaughlan, D. M. J. Cowell, and S. Freear, "Superharmonic imaging with chirp coded excitation: Filtering spectrally overlapped harmonics," *Ultrasonics, Ferroelectrics and Frequency Control, IEEE Transactions on*, vol. 61, no. 11, pp. 1802–1814, 2014.

[9] A. Bouakaz, B. J. Krenning, W. B. Vletter, F. J. ten Cate, and N. de Jong, "Contrast superharmonic imaging: A feasibility study," *Ultrasound in Medicine & Biology*, vol. 29, no. 4, pp. 547–553, 2003.

[10] E. Biagi, L. Breschi, E. Vannacci, and L. Masotti, "Multipulse technique exploiting the intermodulation of ultrasound waves in a nonlinear medium," *Ultrasonics, Ferroelectrics and Frequency Control, IEEE Transactions on*, vol. 56, no. 3, pp. 520–535, 2009.

[11] C. Tremblay-Darveau, R. Williams, L. Milot, M. Bruce, and P. Burns, "Combined perfusion and doppler imaging using plane-wave nonlinear detection and microbubble contrast agents," *Ultrasonics, Ferroelectrics, and Frequency Control, IEEE Transactions on*, vol. 61, no. 12, pp. 1988–2000, 2014.

[12] A. Sridharan, J. Eisenbrey, P. Machado, H. Ojeda-Fournier, A. Wilkes, A. Sevrukov, R. Mattrey, K. Wallace, C. Chalek, K. Thomenius, and F. Forsberg, "Quantitative analysis of vascular heterogeneity in breast lesions using contrast-enhanced 3-d harmonic and subharmonic ultrasound imaging," *Ultrasonics, Ferroelectrics, and Frequency Control, IEEE Transactions on*, vol. 62, no. 3, pp. 502–510, 2015.

[13] P. Marmottant, S. van der Meer, M. Emmer, M. Versluis, N. de Jong, S. Hilgenfeldt, and D. Lohse, "A model for large amplitude oscillations of coated bubbles accounting for buckling and rupture," *The Journal of the Acoustical Society of America*, vol. 118, no. 6, pp. 3499–3505, 2005.

[14] S. Harput, "Use of chirps in medical ultrasound imaging," Ph.D. Thesis, School of Electronic and Electrical Engineering, University of Leeds, UK, 2012.

[15] T. Misaridis and J. A. Jensen, "Use of modulated excitation signals in medical ultrasound. part i: Basic concepts and expected benefits," *Ultrasonics, Ferroelectrics and Frequency Control, IEEE Transactions on*, vol. 52, no. 2, pp. 177–191, 2005.

[16] D. Y. Kim, J. C. Lee, S. J. Kwon, and T. K. Song, "Ultrasound second harmonic imaging with a weighted chirp signal," in *IEEE Ultrasonics Symposium*, 2001, pp. 1477–1480.

[17] R. Arshadi, A. C. H. Yu, and R. S. C. Cobbold, "Coded excitation methods for ultrasound harmonic imaging," *Canadian Acoustics*, vol. 35, no. 2, pp. 35–46, 2007.

[18] D. M. J. Cowell, P. R. Smith, and S. Freear, "Phase-inversion-based selective harmonic elimination (PI-SHE) in multi-level switched-mode tone- and frequency- modulated excitation," *Ultrasonics, Ferroelectrics and Frequency Control, IEEE Transactions on*, vol. 60, no. 6, pp. 1084–1097, 2013.

[19] Y. Sun, D. E. Kruse, and K. W. Ferrara, "Contrast imaging with chirped excitation," *Ultrasonics, Ferroelectrics and Frequency Control, IEEE Transactions on*, vol. 54, no. 3, pp. 520–529, 2007.

[20] S. Harput, T. Evans, N. Bubb, and S. Freear, "Diagnostic ultrasound tooth imaging using fractional Fourier transform," *Ultrasonics, Ferroelectrics and Frequency Control, IEEE Transactions on*, vol. 58, no. 10, pp. 2096–2106, 2011.

[21] S. Harput, M. Arif, J. McLaughlan, D. M. J. Cowell, and S. Freear, "Extraction of spectrally overlapped second harmonic using the fractional fourier transform," in *Ultrasonics Symposium (IUS), 2013 IEEE International*, 2013, pp. 1501–1504.